



Contents lists available at SciVerse ScienceDirect

## Journal of Discrete Algorithms

[www.elsevier.com/locate/jda](http://www.elsevier.com/locate/jda)

## Monomer-dimer tatami tilings of square regions

Alejandro Erickson<sup>a,\*</sup>, Mark Schurch<sup>b</sup><sup>a</sup> Department of Computer Science, University of Victoria, V8W 3P6, Canada<sup>b</sup> Mathematics and Statistics, University of Victoria, V8W 3R4, Canada

## ARTICLE INFO

## Article history:

Available online 3 April 2012

## Keywords:

Tatami  
Monomer-dimer tiling  
Combinatorial generation  
Gray code  
Enumeration  
Polyomino

## ABSTRACT

We prove that the number of monomer-dimer tilings of an  $n \times n$  square grid, with  $m < n$  monomers in which no four tiles meet at any point is  $m2^m + (m + 1)2^{m+1}$ , when  $m$  and  $n$  have the same parity. In addition, we present a new proof of the result that there are  $n2^{n-1}$  such tilings with  $n$  monomers, which divides the tilings into  $n$  classes of size  $2^{n-1}$ . The sum of these tilings over all monomer counts has the closed form  $2^{n-1}(3n - 4) + 2$  and, curiously, this is equal to the sum of the squares of all parts in all compositions of  $n$ . We also describe two algorithms and a Gray code ordering for generating the  $n2^{n-1}$  tilings with  $n$  monomers, which are both based on our new proof.

© 2012 Elsevier B.V. All rights reserved.

## 1. Introduction

Tatami mats are a traditional Japanese floor covering, whose outside is made of soft woven rush straw, and whose core is stuffed with rice straw. They have been in use by Japanese aristocracy since the 12th century, and are so integral to Japanese culture, that they are often used to describe the square footage of a room. A standard full mat measures  $6' \times 3'$ , and a half mat is  $3' \times 3'$ .

A *dimer* is a  $1 \times 2$  or  $2 \times 1$  tile and a *monomer* is a  $1 \times 1$  tile, used to describe full mats and half mats, respectively. An arrangement of the mats in which no four meet at any point is often preferred, and we call the corresponding tilings of a rectangular grid, monomer-dimer *tatami tilings*. The monomer-dimer tiling in Fig. 1 violates the tatami condition, and the one in Fig. 2 does not.

Tilings with polyominoes are well studied, and they appear in physical models, the theory of regular languages, and combinatorics (see [2,14,7,11,8]).

It is natural to ask, given a room's size, how many different arrangements of mats are there? Motivated by an exercise posed by Knuth [10], Ruskey and Woodcock published the ordinary generating functions for fixed height, dimer-only tatami tilings in [13].

In Fall 2009 our research group discovered the structure which is published in [5], and described in Section 1.1. Problems such as the enumeration of tatami tilings with  $r$  rows,  $c$  columns, and  $m$  monomers, have since become within reach. This paper completes such an enumeration for square grids.

Alhazov et al. followed up on the aforementioned dimer-only research with a treatment of odd-area tatami tilings which include a single monomer. They closed [1] with this remark:

However, the variety of tilings with arbitrary number of monominoes is quite “wild” in sense that such tilings cannot be easily decomposed, see Fig. 11; therefore, most results presented here do not generalize to arbitrary number of

\* Corresponding author.

E-mail addresses: [ate@uvic.ca](mailto:ate@uvic.ca) (A. Erickson), [mschurch@uvic.ca](mailto:mschurch@uvic.ca) (M. Schurch).URL: <http://alejandroerickson.com> (A. Erickson).

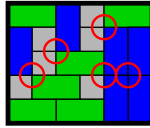


Fig. 1. The tatami condition is that no four tiles may meet at a point. All such violations are circled.

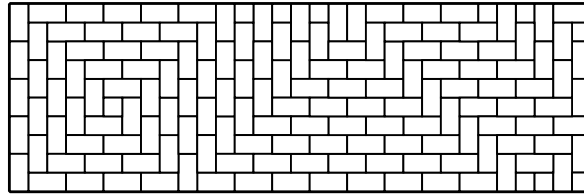


Fig. 2. A tatami tiling of the  $10 \times 31$  grid with 10 monomers, 64 vertical dimers and 86 horizontal dimers. Compare this with Fig. 5.

monominoes, the techniques used here are not applicable, and it is expected that any characterization or enumeration of them would be much more complicated.

The structure we found, however, reveals the opposite; the tilings with an arbitrary number of monomers *are* easily decomposed. The decomposition has a satisfying symmetry, it is amenable to inductive arguments, and it shows that the complexity of a tatami tiling is linear in the dimensions of the grid (compare Fig. 2 with Fig. 5). We use it extensively to prove our main result. Let  $T(n, m)$  be the number of  $n \times n$  tatami tilings with exactly  $m$  monomers.

**Theorem 1.** *If  $n$  and  $m$  have the same parity, and  $m < n$ , then  $T(n, m) = m2^m + (m + 1)2^{m+1}$ .*

This confirms Conjecture 3 in [5] for  $d = 0$  (as was promised there), and completes the enumeration of tatami tilings of square grids, since  $T(n, m) = 0$  when  $m > n$  [5], and trivially when the parities of  $n$  and  $m$  differ.

The proof in [5] that  $T(n, n) = n2^{n-1}$  counts tilings recursively. Due to the symmetry of the solution it is natural to search for a way to divide the tilings into  $n$  classes of size  $2^{n-1}$ ; indeed, Knuth mentioned this in a correspondence with Ruskey, quoted in [6]. We remedy the lack of symmetry in the original proof by presenting a new one which includes the desired partition and counts the tilings directly, rather than recursively.

Nice round numbers such as these tend to be easily identified in output generated by exhaustively listing all tilings on a given size of grid. In a personal communication Ruskey, Knuth noted there appeared to be  $2^{n-1}(3n - 4) + 2$  tatami tilings of the  $n \times n$  grid (see [6]). We prove this result, and show that it is equal to the sum of the squares of all parts in all compositions of  $n$ .

In Section 3 we use the partition in Theorem 2 to exhaustively generate all  $n \times n$  tilings with  $n$  monomers, for even  $n$ , in a constant amount of time per tiling. The problem of generating the tilings in each of these partitions reduces to generating all bit strings of a fixed length, so our first algorithm is a straightforward application of this. The second algorithm generates the tilings in a Gray code order, where the Gray code operation is the diagonal flip (defined in Section 1.1). This is achieved by generating the partitions in a certain order, and using a binary reflected Gray code to generate the bit strings.

### 1.1. Structure

Tatami tilings of rectangular grids have an underlying structure, called the *T-diagram*, which is an arrangement of four possible types of *features*, shown in Figs. 3–4, up to rotation and reflection (see [5] for a complete explanation). Each feature consists of a *source*, shown in colour, which forces the placement of up to four *rays*. Rays propagate to the boundary of the grid and do not intersect each other.

Fig. 3 shows a *loner* and a *vee*, the two features whose sources appear on the boundary of the grid. Fig. 4 depicts a *bidimer* and a *vortex*, and their sources can appear anywhere inside the grid. A bidimer with vertical dimers at its center is called a *vertical bidimer*, and otherwise it is a *horizontal dimer*. Similarly, we call the vortex shown in Fig. 4(b) a *counterclockwise vortex* and its reflection is a *clockwise vortex*.

The placement of a non-zero number of features determines a tiling uniquely if it exists. A T-diagram with no features corresponds to the four ways of laying the tiles in a running bond pattern (brick laying pattern).

Monomers occur on the boundary of the grid, and inside vortices, but nowhere else. The T-diagram is also a partition of the tiles into blocks of horizontal and vertical running bond. The tiling in Fig. 5 uses all four types of features, displays this partition into horizontal and vertical running bond. Its T-diagram is shown on its own in Fig. 6.

Throughout this paper we consider tilings on the  $n \times n$  integer grid, with the origin at the bottom left of the tiling. Let the coordinate of a grid square be the point at its bottom left corner as well.

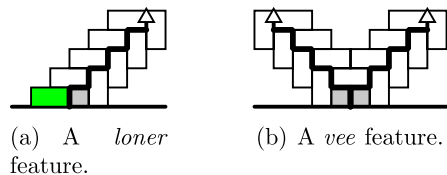


Fig. 3. These two types of features must have their coloured tiles on a boundary, as shown, up to rotation and reflection. (For interpretation of the references to colour in this figure legend, the reader is referred to the web version of this article.)

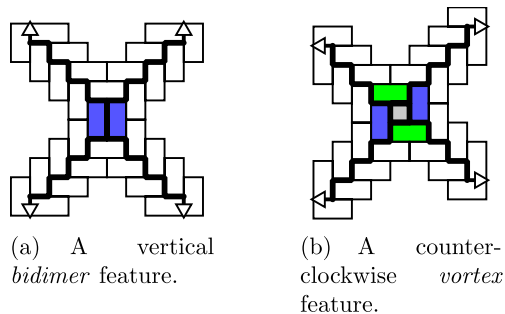


Fig. 4. These two types of features may appear anywhere in a tiling provided that the coloured tiles are not outside the boundaries of the grid. (For interpretation of the references to colour in this figure legend, the reader is referred to the web version of this article.)

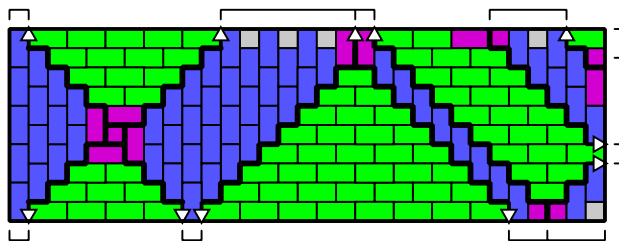


Fig. 5. A tiling showing all four types of sources. Coloured in magenta, from left to right they are, a clockwise vortex, a vertical bidimer, a loner, a vee, and another loner. (For interpretation of the references to colour in this figure legend, the reader is referred to the web version of this article.)

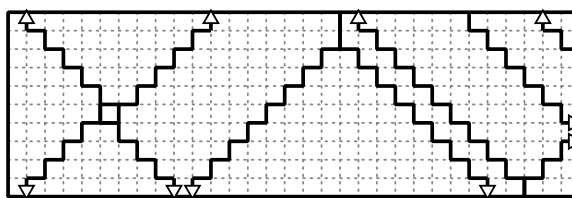


Fig. 6. A T-diagram.

A *diagonal* is a rotation of the following: a monomer at  $(x_0, 0)$ , and (vertical) dimers covering the pairs of grid squares  $(x_0 + 1 + k, k)$  and  $(x_0 + 1 + k, k + 1)$ , for each non-negative  $k$  such that  $x_0 + 1 + k \leq n - 1$ . A diagonal can be *flipped* in place, so that the monomer moves to  $(n - 1, n - x_0 - 1)$ , and the dimers change orientation. This operation preserves the tatami condition. Diagonals are used and illustrated frequently in the next section.

## 2. Square grids

Let  $T_{n,m}$  be the set of  $n \times n$  tatami tilings with  $m$  monomers. To find  $|T_{n,m}|$ , we use a setup similar to that of Theorem 2 in [5]. These lemmas on the composition of such tilings seem apparent from Figs. 7–9, but we prove them in general.

We show that any tiling in  $T_{n,m}$  with  $m < n$  has exactly one bidimer or vortex and we give a one-to-one correspondence between  $m$  and the shortest distance from this source to the boundary. Such a feature determines all tiles in the tiling except a number of diagonals that can be flipped independently. Proving the result becomes a matter of counting the number of allowable positions for the bidimer or vortex, each of which contributes a power of 2 to the sum.

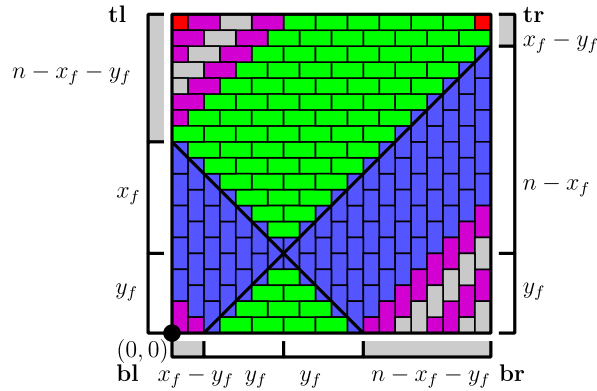


Fig. 7. Vertical bidimer. (For interpretation of the references to colour in this figure, the reader is referred to the web version of this article.)

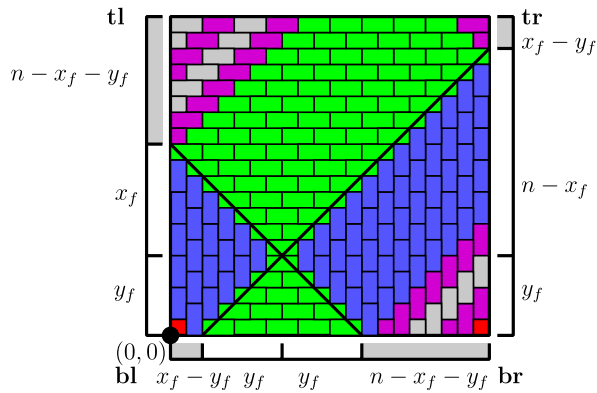


Fig. 8. Horizontal bidimer.

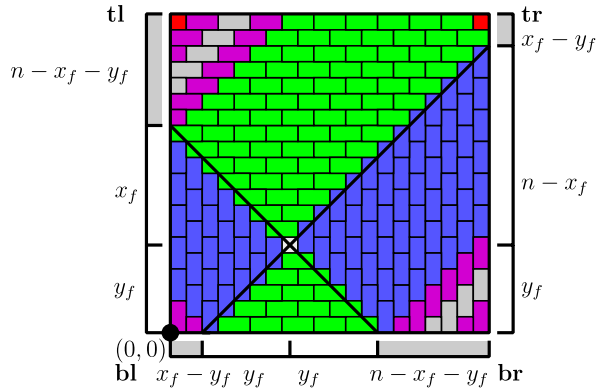


Fig. 9. Counterclockwise vortex. Note that  $x_f$  and  $y_f$  are not integers.

For example, the  $20 \times 20$  tiling in Fig. 7 has a vertical bidimer which forces the placement of the green and blue tiles, while the remaining diagonals are coloured in alternating grey and magenta. There are eight such diagonals, so there are  $2^8$  tilings of the  $20 \times 20$  grid, with a vertical bidimer in the position shown. Each of these  $2^8$  tilings has exactly 10 monomers.

By Corollary 1 in [5], a tiling in  $T_{n,m}$ , with  $m < n$ , must have at least one bidimer or vortex, which we will call  $f$ . Let  $(x_f, y_f)$  be the center of  $f$  in the cartesian plane, where the bottom left of the  $n \times n$  tiling is at the origin.

Define  $X_f$  as the lines  $(x - x_f) + (y - y_f) = 0$  and  $(x - x_f) - (y - y_f) = 0$ , bounded by the grid boundary, which form an X through  $(x_f, y_f)$  (see Figs. 7–9).

Without loss of generality, we may re-orient a tiling, by rotating and reflecting, so that  $y_f \leq x_f \leq n/2$ . The upper arms of  $X_f$  intersect the left and right boundaries of the grid, while the lower arms intersect the bottom. In this range, the distance from this feature to the boundary of the grid is  $y_f$ .

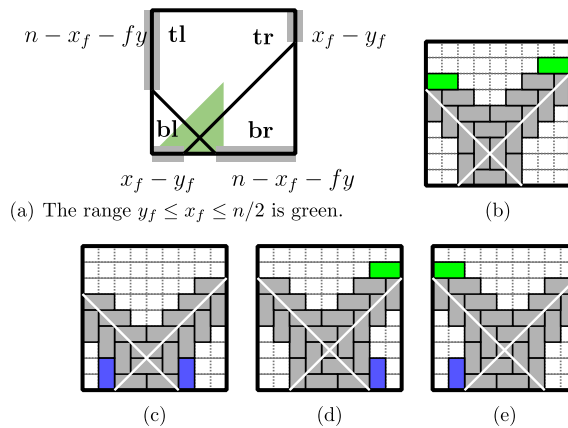


**Fig. 10.** The segments **tl**, **tr**, **bl**, and **br**. When **tl** and **br** have positive length, one of their combined tiles is part of a ray of  $f$ , shown in green or blue. Similarly for **tr** and **bl** combined. (For interpretation of the references to colour in this figure legend, the reader is referred to the web version of this article.)

**Lemma 1.** Let  $T \in \mathbf{T}_{n,m}$ , with  $m < n$ . Then  $T$  has exactly one bidimer or vortex,  $f$ , but not both, and no vees.

**Proof.** It is easy to see that if  $a$  is another bidimer or vortex in the tiling, then  $X_a$  intersects  $X_f$ , which contradicts the fact that rays do not cross. A vee has the same rays as a bidimer, by replacing the adjacent monomers with a dimer, so the only features that may appear, besides  $f$ , are loners.  $\square$

Let  $T_f$  be the tiling with  $f$  as its only feature. This corresponds to the featureless “trivial” tilings in [5].

**Lemma 2.** The tiling  $T_f$  can be obtained from any tiling containing the feature  $f$  via a finite sequence of diagonal flips in which each monomer moves at most once. Reversing this sequence gives the original tiling.

**Proof.** This is a simple modification of the proof of Lemma 3 in [5].  $\square$

**Lemma 3.** All the diagonals in  $T_f$  can be flipped independently.

**Proof.** We show that no two diagonals intersect, by sharing a monomer, or other grid squares.

Let  $\alpha$  and  $\beta$  be the monomers in distinct diagonals, possibly with  $\alpha = \beta$ , which intersect. Let  $L_\alpha$  be the line through  $\alpha$ , and let  $L_\beta$  be the line through  $\beta$ . Their slopes must differ, because in sharing grid squares, they must share whole tiles. Thus we may assume that  $L_\alpha$  has slope 1, and  $L_\beta$  has slope  $-1$ . Then  $L_\alpha$  and  $L_\beta$  intersect inside the grid, and therefore at least one of them intersects with  $X_f$ , which makes the corresponding diagonal unflippable. Therefore distinct diagonals may not intersect.  $\square$

The crux of the argument in Theorem 1 is this:

**Lemma 4.** If  $T_f \in \mathbf{T}_{n,m}$ , with  $y_f \leq x_f \leq n/2$ , then  $m = n - 2y_f$  if  $f$  is a bidimer, and  $m = n - y_f + 1$  if  $f$  is a vortex. The number of (flippable) diagonals in  $T_f$  is

$$\begin{cases} n - 2y_f - 2, & \text{if } y_f < x_f; \\ n - 2y_f - 1, & \text{if } y_f = x_f < n/2; \text{ and} \\ 0, & \text{otherwise.} \end{cases}$$

**Proof.** Let **tl**, **tr**, **bl**, and **br** be the segments of the boundary of the grid delimited by  $X_f$ , as shown in grey in Fig. 10(a). We count the number of monomers and diagonals in  $T_f$  by measuring the lengths of **tl**, **tr**, **bl**, and **br**, minus the tiles in the rays of  $f$ , classified in Figs. 10(b)–(e).

Figs. 10(b)–(e) show (in general) that if **tl** and **br** are non-zero, then together they contain exactly one grid square covered by the ray of  $f$ . The same is true of **tr** and **bl**.

Because of the above, non-zero **tl** and **br** differ in parity, so their sum is odd, and therefore they must contain exactly one corner monomer (which is not in a diagonal). Similarly for **tr** and **bl**.

We tabulate the numbers of monomers and diagonals in **tl**, **tr**, **bl** and **br** for different  $(x_f, y_f)$  in Table 1, and add pairs of rows to prove each case of the theorem statement.

**Table 1**

The number of diagonals and monomers in each corner for different positions,  $(x_f, y_f)$ , of a vortex or bidimer.

$(x_f, y_f)$	Positions	Monomers	Diagonals
$y_f = x_f$	<b>bl</b> and <b>tr</b>	0	0
$y_f < x_f$	<b>bl</b> and <b>tr</b>	$x_f - y_f$	$x_f - y_f - 1$
$y_f = x_f = n/2$	<b>tl</b> and <b>br</b>	0	0
$y_f + x_f < n$	<b>tl</b> and <b>br</b>	$n - x_f - y_f$	$n - x_f - y_f - 1$

**Table 2**

Horizontal, vertical, counterclockwise and clockwise are abbreviated as h, v, cc and c, respectively. We assume  $m > 0$  if  $f$  is a bidimer, and  $m > 1$  if  $f$  is a vortex.

Type	Feature	Positions	Diagonals
$x_f = y_f$	h and v bidimers	4	$m - 1$
$x_f = y_f$	cc and c vortices	4	$m - 2$
$x_f < y_f$	h and v bidimers	$4(m - 1)$	$m - 2$
$x_f < y_f$	cc and c vortices	$4(m - 2)$	$m - 3$

If  $y_f < x_f$ , then  $m = x_f - y_f + n - x_f - y_f = n - 2y_f$  if  $f$  is a bidimer, and  $m = n - 2y_f + 1$  if  $f$  is a vortex. The number of diagonals is  $n - 2y_f - 2$ , as required for this case.

If  $y_f = x_f < n/2$ , then  $m = 0 + n - y_f - y_f = n - 2y_f$  if  $f$  is a bidimer, and  $n - 2y_f + 1$  if  $f$  is a vortex. The number of diagonals is  $n - 2y_f - 1$ .

If  $y_f = x_f = n/2$ , then  $m = 0$  if  $f$  is a bidimer, and  $m = 1$  if it is a vortex. The number of diagonals is 0. □

We sum up the number of positions which give a particular  $m$  in Lemma 4, to count all such tilings.

**Theorem 1.** *If  $n$  and  $m$  have the same parity, and  $m < n$ , then  $T(n, m) = m2^m + (m + 1)2^{m+1}$ .*

**Proof.** We count the number of tilings  $T_f$  in  $\mathbf{T}_{n,m}$ , for each bidimer or vortex,  $f$ , satisfying the conditions of Lemma 4, and for each of these we count the tilings obtainable via a set of (independent) diagonal flips.

If  $f$  is a bidimer, then  $m = n - 2k$ , where  $k$  is the shortest distance from  $(x_f, y_f)$  to the boundary of the grid. These are the positions

$$(k, k), (k, k + 1), (k, k + 2), \dots, (k, n - k), (k + 1, n - k), \dots,$$

$$(n - k, n - k), (n - k, n - k - 1), \dots, (n - k, k), (n - k - 1, k), \dots (k + 1, k),$$

of which there are  $4(n - k - k)$ . We apply Lemma 4 by making the necessary rotations and reflections, so that when  $m > 0$ , the four positions  $(k, k)$ ,  $(k, n - k)$ ,  $(n - k, n - k)$  and  $(n - k, k)$ , have  $m - 1$  diagonals, while the remaining  $4m - 4$  positions have  $m - 2$  diagonals.

The same logic applies when  $f$  is a vortex and  $m > 1$ , and the results are in Table 2.

By Lemmas 2 and 3, all of the tilings which contain  $f$  can be obtained from  $T_f$  by making a set of independent flips. Thus, the number of these is  $2^{d(f)}$ , where  $d(f)$  is the number of diagonals in  $T_f$ .

Lemma 1 tells us that there is no other way to obtain a tiling in  $\mathbf{T}_{n,m}$ , so we conclude by summing the  $2^{d(f)}$ s for each  $f$  such that  $T_f \in \mathbf{T}_{n,m}$ . Each term in the following sum comes from a row of Table 2, in the same respective order, and similarly, the three factors in each sum term come from the last three columns of the table.

$$T(n, m) = 2 \cdot 4 \cdot 2^{m-1} + 2 \cdot 4 \cdot 2^{m-2} + 2 \cdot 4(m - 1) \cdot 2^{m-2} + 2 \cdot 4(m - 2) \cdot 2^{m-3}$$

$$= 2 \cdot 2^{m+1} + 2 \cdot 2^m + (m - 1)2^{m+1} + (m - 2)2^m$$

$$= m2^m + (m + 1)2^{m+1}.$$

That is, there are  $m2^m$  tilings with vortices and  $(m + 1)2^{m+1}$  with bidimers. This also satisfies  $T(n, 0)$  when  $f$  is a bidimer, and  $T(n, 1)$  when  $f$  is a vortex. □

This completes the enumeration of  $n \times n$  tatami tilings with  $m$  monomers.

We present an alternate proof of Theorem 2 in [5]. The new proof organizes the  $n \times n$  tatami tilings with  $n$  monomers into  $n$  classes of size  $2^{n-1}$ , answering a challenge of Knuth, as noted in [6]. In addition to showing a satisfying symmetry, the resulting partition is used in Section 3 for exhaustively generating all such tilings in constant amortized time.

The proof in [5] uses induction on the dimensions of the grid to show that  $n2^{n-1} = 4S(n)$ , where

$$S(n) = 2^{n-2} + 4S(n - 2), \quad \text{where } S(1) = \frac{1}{4} \text{ and } S(2) = 1.$$

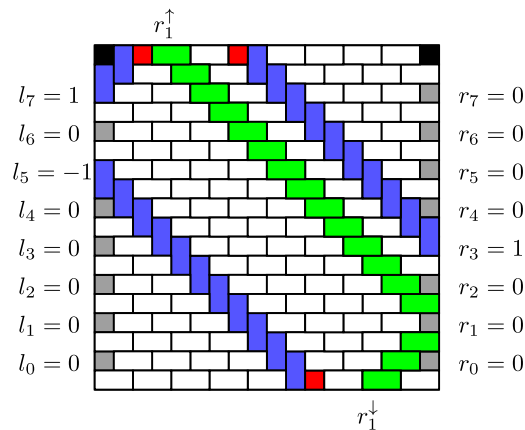


**Fig. 11.** This  $18 \times 18$  tiling is represented by  $(0, 0, 0, 0, 0, -1, 0, 1) \cdot (0, 0, 0, 1, 0, 0, 0, 0)$ . The position of a monomer in the trivial tiling reveals the number of dimers in its diagonals. The flipped diagonals are blue, and the diagonals  $r_1^\uparrow$  and  $r_1^\downarrow$  are green, but they are unflipped. As expected,  $d_{18}(r_1^\downarrow) + d_{18}(r_1^\uparrow) = 3 + 14 = 18 - 1$ . (For interpretation of the references to colour in this figure legend, the reader is referred to the web version of this article.)

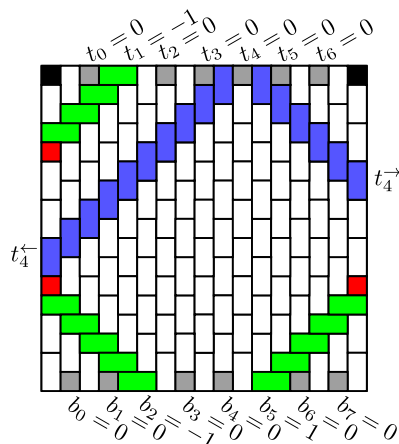


**Fig. 12.** This  $17 \times 17$  tiling is represented by  $(0, -1, 0, 0, 0, 0, 0) \cdot (0, 0, -1, 0, 0, 1, 0, 0)$ . The flipped diagonals are green, and the two blue diagonals are coloured to show  $t_4^\leftarrow$  and  $t_4^\rightarrow$ , which are the left and right diagonals of the same monomer. As expected,  $d_{17}(t_4^\leftarrow) + d_{17}(t_4^\rightarrow) = 10 + 6 = 17 - 1$ . (For interpretation of the references to colour in this figure legend, the reader is referred to the web version of this article.)

The recurrence arises from relating the conflicts in flipping pairs of diagonals in an  $(n - 2) \times (n - 2)$  tiling with those of an  $n \times n$  tiling.

We reuse the setup in [5]. Every tatami tiling of the  $n \times n$  grid with  $n$  monomers can be obtained by performing a sequence of flips (of diagonals) on a running bond, in which no monomer is moved more than once, and the corner monomers remain fixed. As an immediate consequence, every tiling has exactly two corner monomers which are in adjacent corners, and as such, it has four distinct rotational symmetries.

Let  $\mathbf{T}_n$  be the  $n \times n$  tilings with  $n$  monomers, whose upper corners have monomers. It is sufficient to divide the  $n2^{n-3}$  tilings of  $\mathbf{T}_n$ , into  $n$  classes of size  $2^{n-3}$ , and then use the rotational symmetries of these to obtain the  $n$  classes of size  $2^{n-1}$  of all the tilings,  $\mathbf{T}_{n,n}$ .

In this context, a *flipped diagonal* or *monomer* refers to one which was flipped from its initial position in the running bond, in the sequence of flips referred to above. Each monomer is in exactly two diagonals in the trivial tiling, and the monomer is flipped at most once, so its status can be described by a ternary symbol (see Fig. 13). If one of these two diagonals is denoted by  $a$ , we may denote the monomer’s other diagonal by  $\bar{a}$ .

Putting these ternary symbols in a list provides a representation for elements of  $\mathbf{T}_n$ , which contains the status of each monomer as either unflipped, or flipped in a given direction. This gives the sequence of flips required to determine the tiling (see Figs. 11–12).

For even  $n$ , let  $L = (l_0, l_1, \dots, l_{\frac{n-2}{2}-1})$  be a ternary string, with  $l_i$  representing the  $i$ th monomer from the bottom, on the left side of the trivial tiling. Assign  $l_i = 0$  if the monomer is not flipped,  $l_i = -1$  if it is flipped down, and  $l_i = 1$  if it is flipped up. The downward diagonal of a monomer is denoted  $l_i^\downarrow$ , and the upward diagonal is  $l_i^\uparrow$ , regardless of whether they

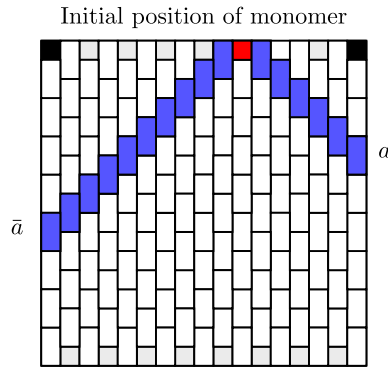


Fig. 13. Each monomer in the trivial tiling is in two diagonals,  $a$  and  $\bar{a}$ . Note that  $d_n(a) + d_n(\bar{a}) = n - 1$ .

Table 3  
Diagonal conflict cases.

A pair of monomers may be	Pair	Conflict 2(b) iff
1. on the same side and flipped		
(a) in the same direction;	$l_i^\downarrow, r_j^\downarrow$	$n \leq 2(i + j) + 2$
(b) away from each other; or	$l_i^\uparrow, r_j^\uparrow$	$n \geq 2(i + j) + 4$
(c) toward each other; or		
2. on different sides and flipped		
(a) in different directions; or	$b_i^{\leftarrow}, t_j^{\leftarrow}$	$n \leq 2(i + j) + 3$
(b) in the same direction.	$b_i^{\rightarrow}, t_j^{\rightarrow}$	$n \geq 2(i + j) + 5$

can, or have been flipped. Similarly, we define  $R = (r_0, r_1, \dots, r_{\lfloor \frac{n-2}{2} \rfloor})$ . Their concatenation,  $L \cdot R$  determines the tiling by describing the diagonal flips, up the left side, then up the right side.

If  $n$  is odd the representation is similar, noting that there are  $\lfloor \frac{n-2}{2} \rfloor$  non-fixed monomers along the top and  $\lceil \frac{n-2}{2} \rceil$  along the bottom. We label from left to right, by  $To = (t_0, t_1, \dots, t_{\lfloor \frac{n-2}{2} \rfloor})$  and  $Bo = (b_0, b_1, \dots, b_{\lceil \frac{n-2}{2} \rceil})$ , respectively, and let  $t_i = -1$  if it is flipped on its left diagonal. Similarly, we define  $t_i^{\rightarrow}$  as the rightward diagonal of  $t_i$ , and so forth.

Let  $d_n(a)$  be the number of dimers in the diagonal  $a$ , also called the length or size of the diagonal. It is a function of the index and direction of  $a$ :

$$d_n(a) = \begin{cases} 2i + 1, & \text{if } a = l_i^\downarrow \text{ or } a = r_i^\downarrow \text{ or } a = b_i^{\leftarrow}; \\ n - 2i - 2, & \text{if } a = l_i^\uparrow \text{ or } a = r_i^\uparrow \text{ or } a = b_i^{\rightarrow}; \\ 2i + 2, & \text{if } a = t_i^{\leftarrow}; \text{ and} \\ n - 2i - 3, & \text{if } a = t_i^{\rightarrow}. \end{cases}$$

Conflicting pairs of diagonal are identified in a constant number of operations by using the cases listed in Table 3. Conflicts occur only in cases 1(c) and 2(b), and case 1(c) is always a conflict. In the case of 2(b), there is a conflict if and only if the sizes of the diagonals sum to at least  $n$ .

Let  $\mathbf{T}_n(a) \subseteq \mathbf{T}_n$ , where  $a$  is a diagonal (one of  $l_i^\downarrow, l_i^\uparrow, r_i^\downarrow, r_i^\uparrow, b_i^{\leftarrow}, b_i^{\rightarrow}, t_i^{\leftarrow}$ , or  $t_i^{\rightarrow}$ ), be defined as the collection of tilings in  $\mathbf{T}_n$  where  $d_n(b) < d_n(a)$ , for each flipped diagonal  $b$ , distinct from  $a$ . That is,  $a$  is strictly the longest flipped diagonal.

Let  $\mathbf{T}_n(\emptyset)$  be the set of tilings for which  $d_n(a) < d_n(\bar{a})$ , for each flipped diagonal  $a$ . That is, each monomer may only be flipped on its strictly shortest diagonal.

Here is the new proof, using the notation defined above.

**Theorem 2.** (See [5].)  $T(n, n) = n2^{n-1}$ .

**Proof.** ( $n$  classes of size  $2^{n-1}$ ) Let  $D$  be the set of diagonals in the trivial tiling. Let  $A = \{a \in D : d_n(a) > d_n(\bar{a})\}$  and let  $\dot{\cup}$  denote a disjoint union. We prove that

$$\mathbf{T}_n = \mathbf{T}_n(\emptyset) \dot{\cup} \left( \dot{\bigcup}_{a \in A} \mathbf{T}_n(a) \right),$$

and, for  $a \in A$ ,

$$\left( |\mathbf{T}_n(a)|, |\mathbf{T}_n(\emptyset)|, |A| \right) = \begin{cases} (2^{n-3}, 2^{n-2}, n - 2), & \text{if } n \text{ is even; and} \\ (2^{n-3}, 2^{n-3}, n - 1), & \text{if } n \text{ is odd,} \end{cases} \tag{1}$$

which gives the correct sizes, since  $|\mathbf{T}_n| = (n - 2)2^{n-3} + 2^{n-2} = (n - 1)2^{n-3} + 2^{n-3}$ .



**Table 4**

Each  $\mathbf{T}_n(a)$  has exactly  $\log_2(|\mathbf{T}_n(a)|)$  independently flippable diagonals. See Figs. 14–15 for examples.

$j$ must satisfy these constraints				
$n$ odd	$t_j^{\leftarrow}$	$t_j^{\rightarrow}$	$b_j^{\leftarrow}$	$b_j^{\rightarrow}$
$\mathbf{T}_n(t_i^{\leftarrow})$	$d_n(t_j^{\leftarrow}) < d_n(t_i^{\leftarrow})$ $\Rightarrow j < i$	conflict 1(c) $\Rightarrow i < j$	conflict 2(b) $\Rightarrow j < \frac{n-3}{2} - i$	$d_n(b_j^{\rightarrow}) < d_n(t_i^{\leftarrow})$ $\Rightarrow j > \frac{n-4}{2} - i$
$\mathbf{T}_n(b_i^{\leftarrow})$	conflict 2(b) $\Rightarrow j < \frac{n-3}{2} - i$	$d_n(t_j^{\rightarrow}) < d_n(b_i^{\leftarrow})$ $\Rightarrow j > \frac{n-4}{2} - i$	$d_n(b_j^{\leftarrow}) < d_n(b_i^{\leftarrow})$ $\Rightarrow j < i$	conflict 1(c) $\Rightarrow i < j$
$\mathbf{T}_n(t_i^{\rightarrow})$	symmetry with $\mathbf{T}_n(t_i^{\leftarrow})$			
$\mathbf{T}_n(b_i^{\rightarrow})$	symmetry with $\mathbf{T}_n(b_i^{\leftarrow})$			
$\mathbf{T}_n(\emptyset)$	$d_n(t_j^{\leftarrow}) < d_n(t_j^{\rightarrow})$ $\Rightarrow j < \frac{n-5}{4}$	$d_n(t_j^{\rightarrow}) < d_n(t_j^{\leftarrow})$ $\Rightarrow j > \frac{n-5}{4}$	$d_n(b_j^{\leftarrow}) < d_n(b_j^{\rightarrow})$ $\Rightarrow j < \frac{n-3}{4}$	$d_n(b_j^{\rightarrow}) < d_n(b_j^{\leftarrow})$ $\Rightarrow j > \frac{n-3}{4}$
$n$ even	$l_j^{\downarrow}$	$l_j^{\uparrow}$	$r_i^{\downarrow}$	$r_i^{\uparrow}$
$\mathbf{T}_n(l_i^{\downarrow})$	$d_n(l_j^{\downarrow}) < d_n(l_i^{\downarrow})$ $\Rightarrow j < i$	conflict 1(c) $\Rightarrow i < j$	conflict 2(b) $\Rightarrow j < \frac{n-2}{2} - i$	$d_n(r_j^{\uparrow}) < d_n(l_i^{\downarrow})$ $\Rightarrow j > \frac{n-3}{2} - i$
$\mathbf{T}_n(l_i^{\uparrow})$	conflict 1(c) $\Rightarrow j < i$	$d_n(l_j^{\uparrow}) < d_n(l_i^{\uparrow})$ $\Rightarrow i < j$	$d_n(r_j^{\downarrow}) < d_n(l_i^{\uparrow})$ $\Rightarrow j < \frac{n-3}{2} - i$	conflict 2(b) $\Rightarrow j > \frac{n-4}{2} - i$
$\mathbf{T}_n(r_i^{\downarrow})$	symmetry with $\mathbf{T}_n(l_i^{\downarrow})$			
$\mathbf{T}_n(r_i^{\uparrow})$	symmetry with $\mathbf{T}_n(l_i^{\uparrow})$			
$\mathbf{T}_n(\emptyset)$	$d_n(l_j^{\downarrow}) < d_n(l_j^{\uparrow})$ $\Rightarrow j < \frac{n-3}{4}$	$d_n(l_j^{\uparrow}) < d_n(l_j^{\downarrow})$ $\Rightarrow j > \frac{n-3}{4}$	$d_n(r_j^{\downarrow}) < d_n(r_j^{\uparrow})$ $\Rightarrow j < \frac{n-3}{4}$	$d_n(r_j^{\uparrow}) < d_n(r_j^{\downarrow})$ $\Rightarrow j > \frac{n-3}{4}$

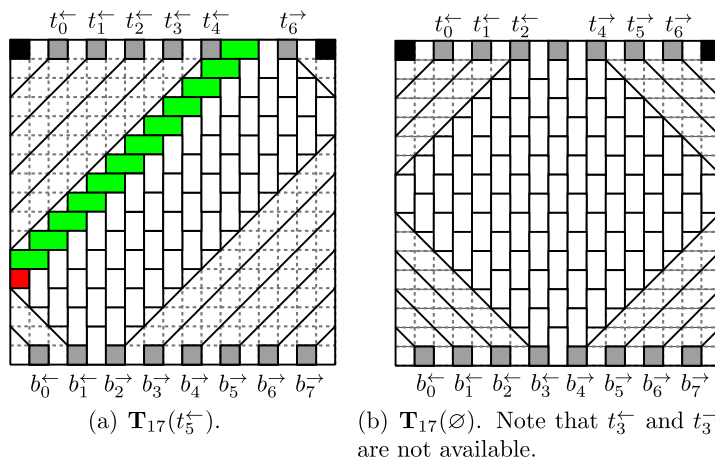


**Fig. 14.** Odd  $n$ . Available diagonals are marked by solid lines.

An *available diagonal* in  $\mathbf{T}_n(a)$  is a diagonal that may be flipped in a tiling of  $\mathbf{T}_n(a)$ , subject to the constraints that  $a \in A \cup \{\emptyset\}$  and if  $a \neq \emptyset$ , then  $d_n(b) < d_n(a)$ , and  $b$  does not conflict with  $a$ .

It suffices to show that the available diagonals are pairwise non-conflicting, and independent, and that for each  $\mathbf{T}_n(a)$ , there are  $\log_2(|\mathbf{T}_n(a)|)$  of them. See Table 4 for all the cases, and Figs. 14–15 for examples.

For odd  $n$ , the diagonals  $a$  and  $\bar{a}$  of the monomer on the middle column are equal in length. Thus it is not flipped at all in  $\mathbf{T}_n(\emptyset)$ , giving the number  $|\mathbf{T}_n(\emptyset)| = 2^{n-3}$ , however,  $a, \bar{a} \in A$ , so  $|A| = n - 1$ .

For even  $n$ , no such symmetry exists, so we have  $|\mathbf{T}_n(\emptyset)| = 2^{n-2}$ , and we must partition  $\mathbf{T}_n(\emptyset)$  into halves to obtain  $n$  classes of size  $2^{n-3}$ .  $\square$

**Corollary 1.** The number of  $n \times n$  tatami tilings is  $2^{n-1}(3n - 4) + 2$ .

**Proof.** By Corollary 1 in [5], we have that  $T(n, m) = 0$  when  $m > n$ . Let  $T(n) = \sum_{m \geq 0} T(n, m)$ , so that

$$T(n) = n2^{n-1} + \sum_{i=1}^{\lfloor n/2 \rfloor} ((n - 2i)2^{n-2i} + (n - 2i + 1)2^{n-2i+1}),$$

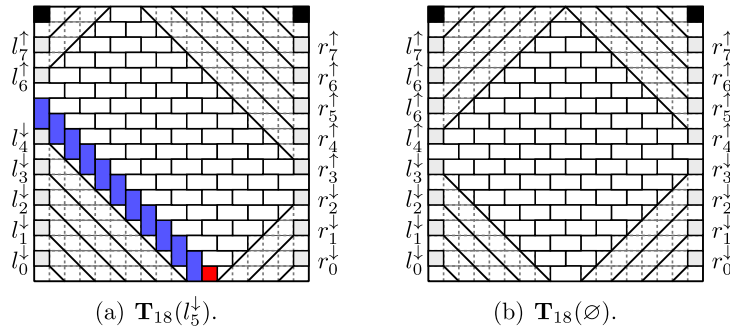


Fig. 15. Even  $n$ . Available diagonals are marked by solid lines.

and notice that the sum simplifies to

$$T(n) = n2^{n-1} + \sum_{i=1}^{n-1} i2^i.$$

Now we use the fact that  $2^k + 2^{k+1} + \dots + 2^{n-1} = 2^n - 1 - 2^k + 1 = 2^n - 2^k$  to rearrange the sum.

$$\begin{aligned} T(n) &= n2^{n-1} + \sum_{i=1}^{n-1} i2^i \\ &= n2^{n-1} + (n-1)2^n - \sum_{i=1}^{n-1} 2^i \\ &= 2^{n-1}(3n-4) + 2. \quad \square \end{aligned}$$

By cross referencing the result of Corollary 1 with the On-Line Encyclopedia of Integer Sequences [9], a surprising correspondence with integer compositions of  $n$  was discovered (see sequence A027992). No proof is included in the sequence reference so we have included one here which illuminates a symmetry in this correspondence.

We restate the result of Theorem 1 in terms of the distance of a bidimer or vortex from the boundary of the grid.

**Lemma 5.** For  $1 \leq k \leq n-1$ , the number of tatami tilings of the  $n \times n$  grid with a vortex or bidimer a distance  $(k+1)/2$  from the boundary is  $(n-k)2^{n-k}$ .

**Proof.** In the proof of Theorem 1 it was shown that the number of tilings of the  $n \times n$  grid with  $m$  monomers and a vortex is  $m2^m$ , and with a bidimer it is  $(m+1)2^{m+1}$ . Let  $d$  be the minimum distance from the center of a feature to the boundary of the grid. By Lemma 4 in the case of a bidimer  $m = n - 2d$  and in the case of a vortex  $m = 2d + 1$ . Thus, in either case, the number of tilings written in terms of  $d$  is  $(n - 2d + 1)2^{n-2d+1}$  or equivalently,  $(n - k)2^{n-k}$  where  $k = 2d - 1$ .  $\square$

**Proposition 1.** The number of  $n \times n$  tatami tilings is equal to the sum of the squares of all parts in all compositions of  $n$ .

**Proof.** Note that the number of red boxes in Fig. 16, is the sum of the squares of all parts in all compositions of 5. We consider in general this visual representation and show that for an integer composition of  $n$  the number of red boxes is equal to the number of tilings of the  $n \times n$  grid. We proceed by partitioning these red boxes into  $n$  classes and showing that the cardinality of each class is equal to the number of tilings with a feature (or no features) a distance  $k/2$  from the edge of the grid, for some  $k \in \{2, 3, \dots, n\}$ .

For each of the  $n \times n$  arrays in Fig. 16, view the top left corner as having the  $(x, y)$  coordinates  $(0, 0)$  and the bottom right corner as having the coordinates  $(n, -n)$ . Now consider a grouping of these red boxes into  $n$  classes, where a box is in class  $X_k$ , for  $0 \leq k \leq n-1$ , whenever its center lies on one of the lines  $y = -x \pm k$ . The number of red boxes in class  $X_0$  is the number of red boxes along the line  $y = -x$ , which is  $n2^{n-1}$  since there are  $2^{n-1}$  compositions of  $n$  and  $n$  red boxes along each central diagonal. By Theorem 2 this is equal to the number of tilings of the  $n \times n$  grid with the maximum number of monomers, or equivalently, no bidimers or vortices.

For  $1 \leq k \leq n-1$ , if a summand of size  $i \geq k$  appears in a composition of  $n$ , then there are  $2(i-k)$  red boxes along the lines  $y = \pm k$  and none if  $i < k$ . In [4] the authors show that the number of summands of size  $1 \leq i < n$  over all compositions

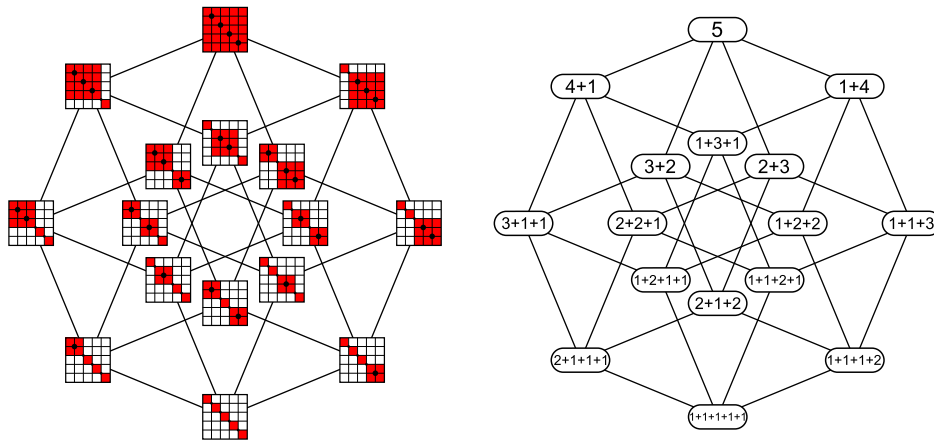


**Fig. 16.** A pictorial representation of the squares of all parts in all compositions of 5 (see [12]). (For interpretation of the references to colour in this figure, the reader is referred to the web version of this article.)

of  $n \geq 2$  is given by  $(n + 3 - i)2^{(n-2-i)}$ , and trivially a summand of size  $n$  occurs once. Thus the number of red boxes in class  $X_k$ , for  $1 \leq k \leq n - 1$ , is

$$2(n - k) + \sum_{i=k+1}^{n-1} (n + 3 - i)(i - k)2^{(n-1-i)}. \tag{2}$$

Expression (2) simplifies to  $(n - k)2^{n-k}$  (details are omitted) which, by Lemma 5, is the number of tilings of the  $n \times n$  grid with a feature a distance  $\frac{k+1}{2}$  from the boundary where  $1 \leq k \leq n - 1$ .  $\square$

### 3. Combinatorial generation algorithms

In this section we describe two combinatorial algorithms for generating all elements of  $\mathbf{T}_n$ , for even  $n$ . Each algorithm is a natural extension of our proof of Theorem 2, and we use the notation and ternary representation described there.

The first combinatorial generation algorithm arises most naturally from our new proof of Theorem 2 (the proof in [5] leads to another, recursive algorithm). For each  $\mathbf{T}_n(a)$ , Table 4 can be used to determine the set of available diagonals. Several constant amortized time (CAT) algorithms exist for generating all subsets, so our algorithm is also CAT.

#### 3.1. Gray code

The second algorithm uses a Gray code whose operation is the diagonal flip, which, in our representation, is equivalent to incrementing or decrementing a single ternary symbol. We use a binary reflected Gray code for each class of size  $2^{n-3}$  tilings, and order the classes so that the last tiling of one class is one flip away from first of the next class. If  $n \equiv 2 \pmod{4}$ , this order begins with

$$\mathbf{T}_n(l_0^\uparrow), \mathbf{T}_n(r_{\frac{n-2}{2}-1}^\downarrow), \mathbf{T}_n(l_1^\uparrow), \mathbf{T}_n(r_{\frac{n-2}{2}-2}^\downarrow), \dots, \mathbf{T}_n(l_i^\uparrow), \mathbf{T}_n(r_j^\downarrow)$$

where  $i$  is the largest integer such that  $d_n(l_i^\uparrow) > d_n(l_i^\downarrow)$ , and  $j$  is the smallest integer such that  $d_n(r_j^\downarrow) > d_n(r_j^\uparrow)$ . The next class is  $\mathbf{T}_n(\emptyset)$ , which is followed by

$$\mathbf{T}_n(r_0^\uparrow), \mathbf{T}_n(l_{\frac{n-2}{2}-1}^\downarrow), \mathbf{T}_n(r_1^\uparrow), \mathbf{T}_n(l_{\frac{n-2}{2}-1}^\downarrow), \dots, \mathbf{T}_n(r_{j-1}^\uparrow), \mathbf{T}_n(l_{i+1}^\downarrow).$$

For example, when  $n = 18$  (see Fig. 11), this order is

$$\mathbf{T}_{18}(l_0^\uparrow), \mathbf{T}_{18}(r_7^\downarrow), \mathbf{T}_{18}(l_1^\uparrow), \mathbf{T}_{18}(r_6^\downarrow), \mathbf{T}_{18}(l_2^\uparrow), \mathbf{T}_{18}(r_5^\downarrow), \mathbf{T}_{18}(l_3^\uparrow), \mathbf{T}_{18}(r_4^\downarrow),$$

and then  $\mathbf{T}_{18}(\emptyset)$ , continuing with

$$\mathbf{T}_{18}(r_0^\uparrow), \mathbf{T}_{18}(l_6^\downarrow), \mathbf{T}_{18}(r_1^\uparrow), \mathbf{T}_{18}(l_6^\downarrow), \mathbf{T}_{18}(r_2^\uparrow), \mathbf{T}_{18}(l_5^\downarrow), \mathbf{T}_{18}(r_3^\uparrow), \mathbf{T}_{18}(l_4^\downarrow).$$

The case where  $n \equiv 0 \pmod{4}$  is similar.

The binary reflected Gray code on  $n$  bits begins with the 0 bit string and ends with  $10^{n-1}$ . We assign 0 to unflipped monomers and 1 to flipped monomers, since there is only one available flip for each flippable monomer. In this way, each  $\mathbf{T}_n(a)$  can be generated by one of the CAT algorithms in [3].

To generate two consecutive classes,  $\mathbf{T}_n(a)$  and  $\mathbf{T}_n(b)$ , they must be separated by exactly one flip. Notice that if  $b \neq \emptyset$  and  $a \neq \emptyset$ , then  $b$  is an available diagonal in  $\mathbf{T}_n(a)$ , since  $a$  and  $b$  are on different sides, in different directions, and  $d_n(b) = d_n(a) - 1$ . In this case, we associate  $b$  with the 1 in the last bit string,  $10^{n-3}$ , of  $\mathbf{T}_n(a)$ , and unflipping  $a$  allows us to begin generating  $\mathbf{T}_n(b)$ . If  $b = \emptyset$ , then the order for the bit string of  $\mathbf{T}_n(a)$  is arbitrary, however,  $\mathbf{T}_n(\emptyset)$  must be generated in reverse, ending with the trivial tiling. If  $a = \emptyset$ , then  $\mathbf{T}_n(\emptyset)$  ends with the trivial tiling, so  $b$  is flipped and  $\mathbf{T}_n(b)$  is generated.

The transitions from  $\mathbf{T}_n(a)$  to  $\mathbf{T}_n(b)$  are done in constant time, so this Gray code generation algorithm for  $\mathbf{T}_n$  runs in constant amortized time by making a sequence of calls to one of the CAT algorithms for generating binary reflected Gray codes in [3].

Two problems remain open in this discussion. Is there a Gray code for  $\mathbf{T}_n$  whose first and last elements also differ by 1 operation? A positive answer would provide a Gray code for  $\mathbf{T}_n^{\text{all}}$ .

Our present discussion is about  $m = n$  and even  $n$ , but much of this applies to tilings of odd dimension or with less than  $n$  monomers.

#### 4. Further research

This paper answers some questions central to the enumeration and exhaustive generation of square monomer-dimer tatami tilings, and similar findings are in preparation for the  $r \times c$  grid, with  $r < c$  (see [5] for related conjectures). The present research opens up the following paths:

- find a useful representation for tilings in  $\mathbf{T}_{n,m}$  which is amenable to making diagonal flips;
- exhaustively generate all of  $\mathbf{T}_{n,m}$  in constant amortized time;
- find the corresponding Gray code of Section 3.1 for odd  $n$ ;
- find an aesthetically pleasing bijection from the  $n \times n$  tatami tilings to the red boxes of Fig. 16, for all  $n$ . Preferably one which uses elements of the proof of Proposition 1; and
- explore  $n \times n$  tilings with exactly  $v$  vertical dimers.

This last point is in preparation, and might have been published here, save for its length. We will give a CAT algorithm for generating all of the  $n \times n$  tatami tilings with exactly  $m$  monomers,  $v$  vertical dimers and  $h$  horizontal dimers, and we will explain the origin of the generating polynomial in Conjecture 4 in [5].

#### Acknowledgements

The authors are grateful to Prof. Frank Ruskey and Prof. Don Knuth for their interest and involvement in tatami tilings. We also thank the anonymous referees, and editors Prof. Bill Smyth and Prof. Costas Iliopoulos.

#### References

- [1] A. Alhazov, K. Morita, C. Iwamoto, A note on tatami tilings, in: Proceedings of the 2009 LA Winter Symposium, in: Mathematical Foundation of Algorithms and Computer Science, vol. 1691, 2009, pp. 1–7.
- [2] K.P. Benedetto, N.A. Loehr, Tiling problems, automata, and tiling graphs, Theoretical Computer Science 407 (2008) 400–411.
- [3] J.R. Bitner, G. Ehrlich, E.M. Reingold, Efficient generation of the binary reflected gray code and its applications, Communications of the ACM 19 (1976) 517–521.
- [4] P. Chinn, G. Colyer, M. Flashman, E. Migliore, Cuisenaire rods go to college, Primus 2 (1992) 118–130.
- [5] A. Erickson, F. Ruskey, M. Schurch, J. Woodcock, Monomer-dimer tatami tilings of rectangular regions, The Electronic Journal of Combinatorics 18 (2011) 24.
- [6] A. Erickson, M. Schurch, Enumerating tatami mat arrangements of square grids, in: 22nd International Workshop on Combinatorial Algorithms (IWOCA), in: Lecture Notes in Computer Science (LNCS), vol. 7056, Springer, Berlin/Heidelberg, 2011, p. 12.
- [7] D. Gale, S.W. Golomb, R. Haas, Mathematical entertainments, The Mathematical Intelligencer 18 (1996) 38–47.
- [8] J.L. Hock, R.B. McQuistan, A note on the occupational degeneracy for dimers on a saturated two-dimensional lattice space, Discrete Applied Mathematics 8 (1984) 101–104.
- [9] V. Jovovic, Comment on A027992, <http://oeis.org/A027992>, 2005.
- [10] D.E. Knuth, The Art of Computer Programming, vol. 4A: Combinatorial Algorithms, Part 1, 1st edition, Addison-Wesley Professional, 2011.
- [11] D. Merlini, R. Sprugnoli, M.C. Verri, Strip tiling and regular grammars, Theoretical Computer Science 242 (2000) 109–124.
- [12] T. Piesk, Binary and compositions 5, [http://commons.wikimedia.org/wiki/File:Binary\\_and\\_compositions\\_5.svg](http://commons.wikimedia.org/wiki/File:Binary_and_compositions_5.svg), 2010.
- [13] F. Ruskey, J. Woodcock, Counting fixed-height tatami tilings, The Electronic Journal of Combinatorics 16 (2009) 20.
- [14] R.P. Stanley, On dimer coverings of rectangles of fixed width, Discrete Applied Mathematics 12 (1985) 81–87.